ELSEVIER

Thermochimica Acta 388 (2002) 129–141

thermochimica acta

www.elsevier.com/locate/tca

Initial crystallization kinetics in undercooled droplets

J.H. Perepezko[a,*], P.G. Höckel[b], J.S. Paik[c]

[a]*Department of Materials Science and Engineering, University of Wisconsin, 1509 University Avenue, Madison, WI 53706, USA*
[b]*Intel Corporation, M/S RA1-329, 5200 N.E. Elam Young Parkway, Hillsboro, OR 97124-6497, USA*
[c]*Korea Standards Research Institute, Taedok, South Korea*

Received 9 July 2001; received in revised form 14 September 2001; accepted 14 September 2001

Abstract

In large liquid volumes a variety of residual catalysts can limit the attainable undercooling. With a liquid droplet dispersion an effective nucleant isolation has yielded the largest undercooling for solidification and conditions where the nucleation process is the rate limiting step. Calorimetric measurements provide an effective means to determine the nucleation frequency in droplet samples. Since droplet samples are polydisperse in size, a full kinetics evaluation requires also a consideration of the size distribution which often obeys a log–normal relationship. With this information, the isothermal solidification rate constants may be determined to distinguish between a volume dependent process and a heterogeneous surface area dependent mechanism. An additional study of heterogeneous nucleation kinetics is possible in droplets containing well-defined solid catalyst surfaces in contact with the liquid which undercool to a clear nucleation onset. Suitable two-phase liquid + solid droplet samples may be generated in eutectic and peritectic alloys following thermal cycling and allow for a further analysis of the rate controlling kinetics. © 2002 Elsevier Science B.V. All rights reserved.

Keywords: Crystallization; Undercooling; Nucleation kinetics; Nucleation catalysis; Calorimetric analysis

1. Introduction

The study of the kinetics of crystallization of undercooled liquids has been an area of continuing interest [1]. While there have been numerous studies of the nucleation kinetics only relatively few have been of sufficient depth to provide the kinetics information needed to model the controlling process. Foremost among these studies has been the classic work on mercury by Turnbull [2]. Succeeding investigations [3,4] on nucleation kinetics have followed essentially a similar analysis technique and method. The results of a detailed kinetics analysis have confirmed the essential form of classical nucleation theory. However, a number of discrepancies have arisen between the predictions of theory and the experimental results. Moreover, theoretical analyses and model simulations of nucleation phenomena continue to attract a strong interest [5–7]. These developments as well as advances in extending the range of maximum undercooling for many metals and alloys [8] point out the need for a further effort in the experimental study of the nucleation kinetics of undercooled liquids.

For the most part the experimental study of the kinetics of crystal nucleation from the highly undercooled liquid state has focused upon the use of a droplet dispersion sample configuration. Turnbull [2] developed the generation of droplets by emulsification of

* Corresponding author. Tel.: +1-608-263-1678; fax: +1-608-262-8353.
E-mail address: perepezk@engr.wisc.edu (J.H. Perepezko).

0040-6031/02/$ – see front matter © 2002 Elsevier Science B.V. All rights reserved.
PII: S0040-6031(02)00022-9

liquid metals in a carrier fluid. To maintain the independence of each droplet, a surface coating was provided in a controlled manner by dissolving a small amount of surfactants in the carrier fluid. With this approach, internal as well as extraneous nucleant effects could be controlled. The improvement of the droplet partitioning technique to develop a less catalytic and stable surface coating has resulted in an extensive amount of undercooling before the onset of copious crystallization for several pure metals [8]. The maximum undercooling results by themselves, however, could not be considered sufficient to prove that the operating nucleation kinetics is the homogeneous nucleation. For the further identification of the controlling nucleation kinetics it was necessary to demonstrate that the nucleation rate is proportional to the liquid droplet volume or droplet surface area.

Under most conditions, solidification is initiated by a heterogeneous nucleation event. While the study of homogeneous nucleation requires a sample free from all external nucleants, the study of heterogeneous nucleation requires a sample which contains only well known and characterized nucleants. A proper examination of nucleation catalysis requires the full identification of the catalytic site and solidification product structure as well as a characterization of the potency of the catalytic site in terms of the interaction energetics (i.e. contact angle) between the nucleus and catalyst. In bulk systems, these requirements are extremely difficult to satisfy with certainty, since there exists a variety of potentially viable heterogeneous sites dispersed throughout the volume. To circumvent the difficulties encountered in bulk systems, a droplet technique has often been utilized to examine nucleation catalysis. Most of the studies have been conducted on binary alloys which are suitable to determine the catalytic effect of a primary solid solution phase on the nucleation of the liquid. For most experimental arrangements, including the droplet technique, contact angles are not possible to measure accurately, but it has been demonstrated [9,10] that each characteristic contact angle between the nucleant and the liquid will yield a discrete, well-defined nucleation undercooling which can be used to describe catalytic potency. An essential component of the experimental approach is the development of an evaluation procedure that allows for the confirmation of specific nucleant site activity [11]. It is important to note that in all other similar types of studies nucleant identity was, for the most part, assumed, rather than confirmed by any experimental test. With an established nucleant identity, careful analysis of the kinetics allows for an evaluation of nucleation site models to be carried out which in turn allows for an assessment of the active site.

The usual methods of generating droplet dispersions involve the production of a distribution in droplet sizes. The analysis requirements associated with droplet distributions and the application of a suitable analysis method are important to the critical examination of nucleation kinetics in undercooled liquids. Similarly, with known nucleation sites an effective model of the catalysis is essential in understanding and controlling the reaction kinetics for heterogeneous nucleation.

1.1. Kinetics analysis model

Droplet samples prepared by emulsification of liquid metals have a size distribution. The nucleation probability of each liquid droplet is proportional to its size. The isothermal solidification rate data of liquid metal droplets, therefore, represents the time dependence of the size distribution of liquid droplets at a given temperature. For the proper analysis of the isothermal solidification kinetics data, the size distribution of liquid droplets must be associated with the experimental measurements [2–4]. A differential scanning calorimetry (DSC) technique, which has advantages in temperature control and sensitivity, has been selected as the basis for the analysis of nucleation rate measurements.

When droplets are produced by shearing, it is expected that due to the random nature of the droplet shearing the droplet size would display a log–normal distribution. For log-normally distributed droplets, the probability distribution [12] is given by

$$P(v_i) = \frac{1}{\sigma_v v_i \sqrt{2\pi}} \exp\left[\frac{-(\ln v_i - \mu_v)^2}{2\sigma_v^2}\right] \quad (1)$$

where v_i is the volume of a droplet belonging to a size group i, σ_v the standard deviation and μ_v the mean value. An example of the log–normal distribution characteristic based upon droplet surface area is presented in Fig. 1 for a Hg droplet emulsion sample.

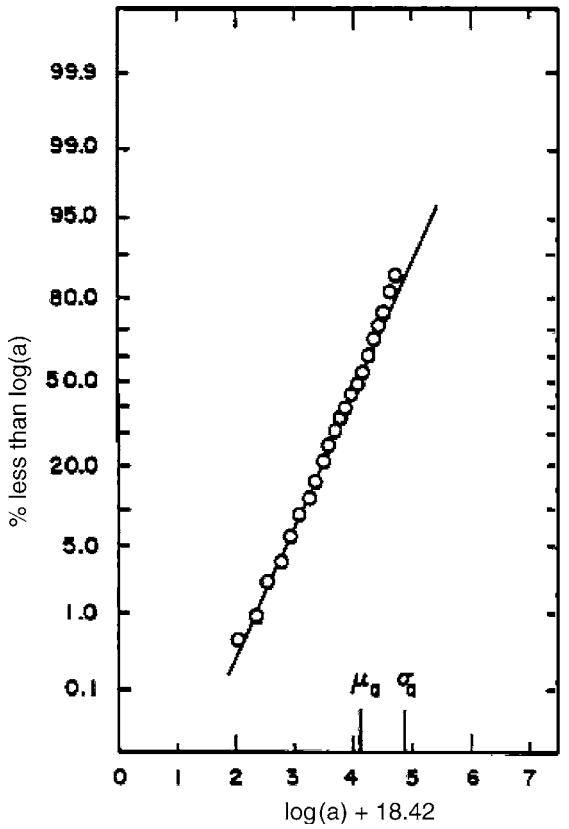

Fig. 1. Cumulative probability plot for surface area distribution in a Hg droplet sample.

When a fine liquid droplet sample is solidified in a highly undercooled condition, the nucleation step becomes a solidification rate determining step [2]. Therefore, the nucleation rate is equivalent to the solidification rate. Since the nucleation event in each droplet of size v_i is a single independent event [2], the first order reaction law can be applied as follows:

$$\frac{dN(v_i,t)}{dt} = -k_i N(v_i,t) \tag{2}$$

where $N(v_i, t)$ is the number of liquid droplets belonging to the ith size group at time t and k_i the nucleation frequency. For a volume dependent homogeneous nucleation, $k_i = J_v v_i$, where J_v is the volume dependent nucleation rate and v_i is the volume of a droplet belonging to the ith size group. For a surface area dependent heterogeneous nucleation, $k_i = J_a a_i$, where J_a is the surface area dependent nucleation rate and a_i the surface area of a droplet belonging to the ith size group.

1.2. Analysis of calorimetric data

When liquid droplets with a size distribution are solidified isothermally, the number of droplets, $N_T(t)$, remaining unfrozen at time t is obtained from the integrated form of Eq. (2), as follows:

$$N_T(t) = \sum_{i=1}^{n} N(v_i, t=0)\exp(-k_i t) \tag{3}$$

and the latent heat contribution of unfrozen droplets is:

$$Q(t) = \Delta H_v \sum_{i=1}^{n} N(v_i, t=0)\exp(-k_i t)v_i \tag{4}$$

where ΔH_v is the heat of crystallization per unit volume. If the liquid droplets are undercooled uniformly to the nucleation rate measuring temperature, T_n, the initial log–normal size distribution can be applied directly to describe the size distribution of liquid droplets during the isothermal nucleation process. The general features of the evolution of the droplet distribution are illustrated schematically in Fig. 2. For a given nucleation rate, the largest droplet sizes freeze first and the distribution mean shifts

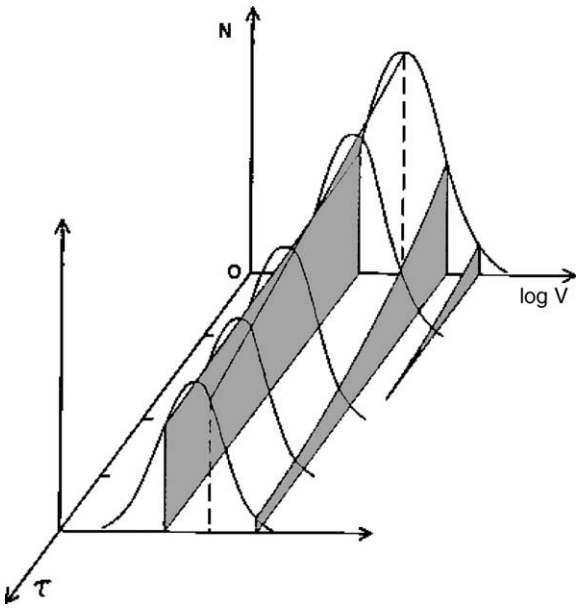

Fig. 2. Illustration of the isothermal nucleation of a droplet population for a volume dependent process.

downward with reaction time. Hence,

$$N(v_i, t=0) = N_T(t=0)P(v_i) \tag{5}$$

where $N_T(t=0)$ is the total number of droplets in a sample. By substituting Eq. (5), $Q(t)$ becomes:

$$Q(t) = \Delta H_v \int_{i=1}^{n} N_T(t=0)P(v_i)\exp(-k_i t)v_i \tag{6}$$

With a DSC method direct measurements can be performed for the isothermal heat liberation rate, $dQ(t)/dt = \dot{Q}$, as a function of time when a droplet sample is held at T_n. Based on the experimental $\dot{Q}$ values the determination of the first derivative of the heat liberation rate, $dQ^2(t)/dt^2 = \ddot{Q}$, and $Q(t)$, is also possible.

1.3. Volume dependent nucleation

For the case of homogeneous nucleation, the nucleation frequency is proportional to the volume of a liquid droplet. Under this condition, Eq. (6) allows $Q(t)$ to be expressed as follows:

$$Q(t) = \Delta H_v N_T(t)\overline{v(t)} \tag{7}$$

where $\overline{v(t)}$ is the first moment of the distribution [12] at time t and $N_T(t)$ the total number of liquid droplets at time t. From Eq. (7), we get

$$\dot{Q} = \Delta H_v(-J_v)\int_{i=1}^{n} N_T(t=0)P(v_i)\exp(-J_v v_i t)v_i^2 \tag{8}$$

$$\dot{Q} = \Delta H_v(-J_v)N_T(t)\overline{[v(t)]^2} \tag{9}$$

where $\overline{[v(t)]^2}$ is the second moment of the distribution [12] at time t related to the undercooled liquid droplets. Experimentally, $\dot{Q}$ values are obtained directly as a function of time by applying a DSC technique. Therefore, the nucleation rate (J_v) can be determined from the experimental $\dot{Q}$ value at a given time and corresponding distribution parameters, $N_T(t)$ and $[v(t)]^2$, which have been determined independently based on the measured droplet size distribution. It is also necessary to measure the first derivative of the heat liberation rate, as follows:

$$\dot{Q} = \Delta H_v(-J_v)^2\int_{i=1}^{n} N_T(t=0)P(v_i)\exp(-J_v v_i t)v_i^3 \tag{10}$$

$$\ddot{Q} = \Delta H_v(-J_v)^2 N_T(t)\overline{[v(t)]^3} \tag{11}$$

where $\overline{[v(t)]^3}$ is the third moment of the distribution [12] at time t related to the undercooled liquid droplets. Experimental $\ddot{Q}$ values represent the instantaneous slope of $\dot{Q}$. Therefore, the volume nucleation rate (J_v) can be determined again from the relevant distribution parameters, $N_T(t)$ and $[v(t)]^3$.

A dimensionless parameter that is useful in distinguishing a volume dependent nucleation from a surface area dependent nucleation can be derived from $Q(t)$, $\dot{Q}$ and $\ddot{Q}$ values as follows:

$$\frac{\ddot{Q}Q(t)}{\dot{Q}^2} = \frac{\overline{[v(t)]^3}\,\overline{[v(t)]}}{\left(\overline{[v(t)]^2}\right)^2} \tag{12}$$

The left-hand side of Eq. (12) is determined experimentally from DSC measurements while the right-hand side is determined by the independent size distribution information. If the equality of Eq. (12) is established from data obtained by the isothermal heat liberation rate measurements on a particular droplet distribution, the nucleation process is controlled by a volume dependent nucleation kinetics.

1.4. Heterogeneous nucleation

One important property of the log–normal distribution is that if the fraction of droplets of any one size is distributed normally on the logarithm of the volume then the fraction of droplets of any one size is distributed normally on the logarithm of any other multiple dimension of the droplet size [12]. It is useful to note that the surface area log–normal distribution parameters are related to the volume distribution parameters by simple relations [12].

$$\mu_a = \tfrac{2}{3}[\mu_v + \log(6\sqrt{\pi})] \tag{13}$$

$$\sigma_a = \tfrac{2}{3}\sigma_v \tag{14}$$

In a heterogeneous nucleation, the nucleation frequency is proportional to the area of the active catalytic site such as the surface of a droplet. Proceeding as for the case of a volume dependent process, the total latent heat of the undercooled liquid droplets at time t, the heat liberation rate, the first derivative of the heat liberation rate and the dimensionless parameter are

given by the following equations:

$$Q(t) = \frac{1}{6\sqrt{\pi}} \Delta H_v N_T(t) \overline{[a(t)]^{3/2}} \quad (15)$$

$$\dot{Q} = \frac{1}{6\sqrt{\pi}} \Delta H_v (-J_a) N_T(t) \overline{[a(t)]^{5/2}} \quad (16)$$

$$\ddot{Q} = \frac{1}{6\sqrt{\pi}} \Delta H_v (-J_a)^2 N_T(t) \overline{[a(t)]^{7/2}} \quad (17)$$

$$\frac{\ddot{Q}Q(t)}{\dot{Q}^2} = \frac{\overline{[a(t)]^{7/2}[a(t)]^{3/2}}}{\left(\overline{[a(t)]^{5/2}}\right)^2} \quad (18)$$

where J_a is now the rate of nucleation per unit area of the droplet surface. The heterogeneous nucleation rate, J_a, can be determined from the experimental $\dot{Q}$ or $\ddot{Q}$ values with relevant distribution parameters once the conditions represented by Eq. (18) are satisfied.

Most often a droplet sample contains a distribution of nucleants either internally or on the droplet surface which can become active during cooling. The droplet fraction which is free of such nucleants can be evaluated from the Poisson distribution function [6]. For example, in a droplet sample containing m_i number of surface catalysts per unit area with droplet volume v_i and corresponding surface area a_i, the fraction, X_1, free of such nucleants is given by:

$$x_i = \exp(-m_i a_i) \quad (19)$$

Under these conditions, the number of liquid droplets of size i that remain in a distribution after cooling from T_m to T_n can be obtained as follows:

$$N(v_i, t) = N_T P(v_i) \exp(-m_i a_i) \exp(-k_i t) \quad (20)$$

where N_T is the total number of droplets and $P(v_i)$ is the log–normal distribution function. The isothermal solidification of a droplet distribution is then described by the total number of unfrozen droplets at t, N_T as the summation of nucleation events over all size classes,

$$N_T(t) = N_T \sum_i P(v_i) \exp(-m_i a_i) \exp(-J_a a_i t) \quad (21)$$

In practice, N_T can be obtained through calorimetric or dilatometric measurements.

As mentioned, it is often found that samples contain multiple nucleation catalysts, but these effects can also be treated on the basis just described. For example, in

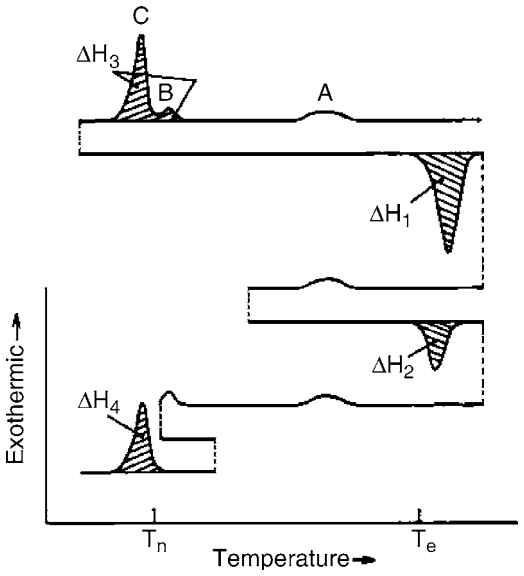

Fig. 3. Series of schematic thermograms for the determination of the fraction of droplet sample solidified in each of three exotherms by a thermal cycling treatment.

Fig. 3 a sample melting at an equilibrium temperature T_e exhibits three crystallization exotherms A, B, and C upon cooling. The procedure is outlined in Fig. 3 to isolate the relative contributions of the droplet population to each of the crystallization exotherms, based upon a Poisson distribution of surface catalytic sites as given in Eq. (19). For example, in dealing with peak A it is possible to assess its relative magnitude in terms of the fraction of the total droplet population, $P(r)$ not containing site A or $P'(r)$ as given by:

$$P'(r) = P(r) \exp(-m_1 a_1) \quad (22)$$

so that

$$\frac{\int_0^\infty V_r P'(r)\,dr}{\int_0^\infty V_r P(r)\,dr} = \frac{\Delta H_1 - \Delta H_2}{\Delta H_1} \quad (23)$$

where V_r is the volume of a droplet with radius r. Similarly for peak B,

$$P''(r) = P'(r) \exp(-m_2 a_2) \quad (24)$$

where a_2 is the catalyst area and

$$\frac{\int_0^\infty V_r P'(r)\,dr}{\int_0^\infty V_r P''(r)\,dr} = \frac{\Delta H_4}{\Delta H_3} \quad (25)$$

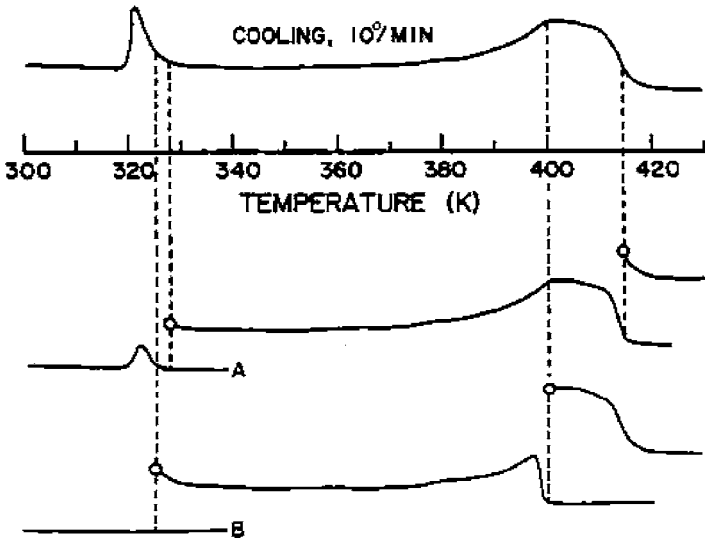

Fig. 4. The influence of thermal cycling and isothermal holding on the undercooling behavior of pure In droplets.

Finally, peak C may be derived by considering the difference between A and B so that the unfrozen droplet fraction at the start of exotherm C is:

$$P''(r) = P(r)\exp(-m_1a_1 - m_2a_2) \tag{26}$$

In this case, the nucleation catalysts exhibited discrete, well-separated exothermic crystallization events, but there are other circumstances which yield a more continuous spectrum of crystallization and catalytic behavior as shown in Fig. 4 for a pure sample. When the cooling process is arrested as shown in curve A of Fig. 4 at a temperature below the melting temperature and the cooling process is restarted, a clear step is observed indicating a series of overlapping crystallization processes terminating in a final crystallization exotherm as shown at the lowest temperature part of curve A. The trace in curve B further illustrates the continuous crystallization and also the fact that the final exotherm at the lowest temperature point is separate from the continuous crystallization. In order to treat the continuous crystallization induced by surface nucleants of variable potency, it is possible to consider regions of surface catalytic sites. The relative potency of these sites can be assessed by noting that the critical nucleus radius, r^* as a function of undercooling ΔT is given by [8]

$$r^*(\Delta T) = \frac{-2\sigma T_m}{\Delta H_v \Delta T} \tag{27}$$

where σ is the liquid-solid interface energy and T_m is the melting temperature. For a surface site of radius $R \geq r^*$, the site can become active when:

$$r^*(\Delta T) = \frac{-\sigma T_m \sin\theta}{\Delta H_v \Delta T} \tag{28}$$

where θ is the contact angle between the nucleated phase and the catalyst. When R is less than r^* embryos can form, but they will not reach the critical nucleus size. Thus, with increasing ΔT, sites of decreasing size become activated in a continuously varying manner. With this approach a continuous heterogeneous nucleation with increasing undercooling can be described and used to separate out any individual crystallization events such as that illustrated in Fig. 4 at maximum undercooling.

1.5. Application of the kinetics analysis

1.5.1. Crystallization at high undercooling

In the application of the analysis model, the size distribution of liquid droplets is determined as a function of the parameter $\tau = Jt$. When $\tau = 0$, the liquid droplet size distribution is log–normal as plotted in Fig. 2 for volume dependent kinetics. As time passes, larger droplets are depleted from the undercooled liquid population faster than smaller ones. Hence, the initial distribution characteristics

of liquid droplets changes as shown in Fig. 2. The resulting size distribution parameters obtained as a function of τ can be associated with experimentally measurable quantities: the total number and volume of liquid droplets at τ is the result of the summation of $N(v_i, \tau)$ and $v_i N(v_i, \tau)$ over all volume elements. The ratio of the total volume at τ to the original volume of the sample gives the volume fraction of liquid at τ, X which is equal to the ratio of the latent heat of the liquid at τ to that originally available at $\tau = 0$. If the experimental dimensionless ratio, $\ddot{Q} \cdot Q(t)/\dot{Q}^2$, is plotted as a function of X, at any nucleation temperature, equivalence with the ratio of appropriate moments of the distribution is required if the mechanism is either a volume or a surface nucleation.

In order to illustrate more clearly the use of the kinetic model an abbreviated summary of the analysis of nucleation in Hg is considered at maximum undercooling [13]. The undercooling and the melting characteristics of an emulsion of mercury droplets produced in a mixed alcohol carrier are presented in Fig. 5 for a 5 °C min^{-1} temperature scanning rate in a Perkin-Elmer DSC-2 or DSC-7. The maximum undercooling to the onset of sensible nucleation is 89 °C which is equivalent to 0.38 T_m and similar to that obtained by Turnbull [14] for volume dependent kinetics. The thermal characteristics displayed in Fig. 5 were possible to maintain in carefully prepared samples during repeated thermal cycles of melting and freezing which are required to determine a temperature dependence of the nucleation rate.

A summary of the thermal treatment schedule followed during each isothermal crystallization rate measurement is presented in Fig. 6. Following step 1, the emulsion is completely liquid and is cooled to a temperature 4 °C above T_n (step 2) to equilibrate the system. In step 3 the sample is quenched to T_n and maintained until the decay of the heat release merges with the baseline. The sample is then cycled in step 4 to above the melting temperature for a succeeding run at a different value of T_n. The additional cycle shown by the dotted trace in Fig. 6 represents the calibration step that is used to ascertain the total heat released during the crystallization, which is essential in order to determine the fraction crystallized with time. The isothermal heat liberation rate as a function of time was measured in a temperature range of 146.5 to 149.2 K over which the nucleation rate becomes experimentally observable (10^7 to 10^{10} nuclei cm^{-3} s^{-1}).

The volume or surface area dependence of the nucleation rate can be determined by comparing the experimental dimensionless ratio value $\ddot{Q} \cdot Q(t)/\dot{Q}^2$,

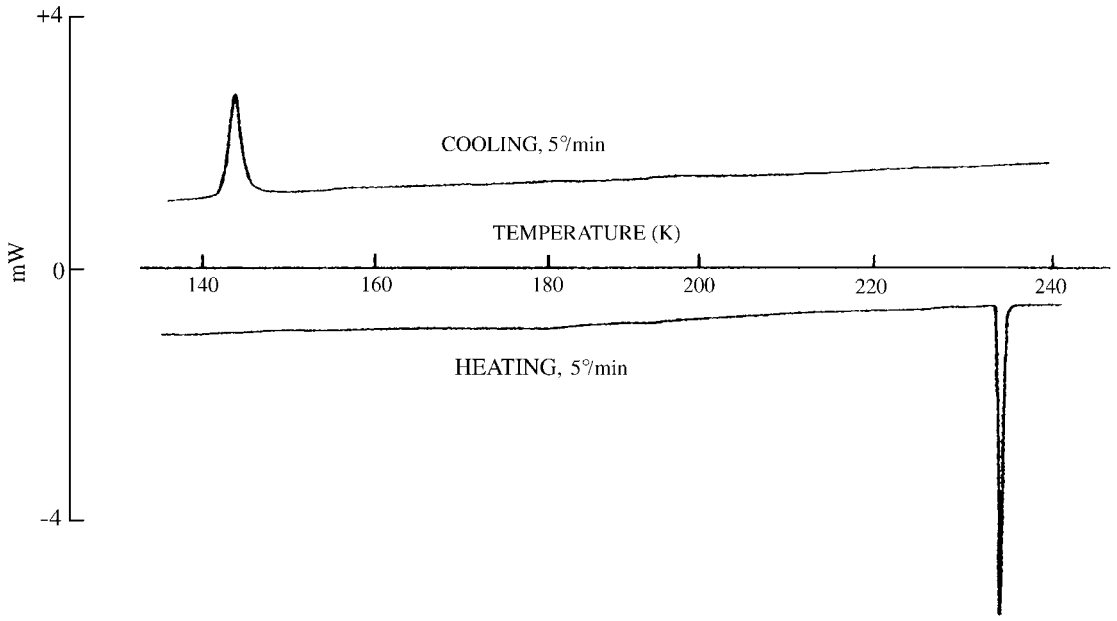

Fig. 5. DSC thermogram of super purity (99.99999%) Hg droplets.

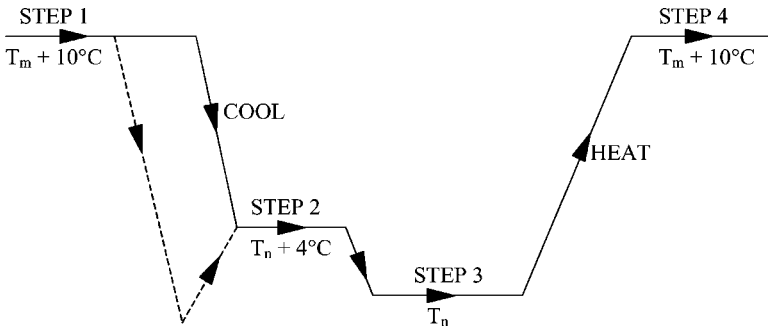

Fig. 6. A summary of the thermal treatment schedule for nucleation rate measurements.

obtained as a function of X with the corresponding ratio value of the appropriate distribution parameters as indicated in Fig. 7. The experimental ratio values were obtained as a function of X based upon calorimetric results while the expected ratio values of distribution parameters are derived from the initial size distribution and the nucleation kinetics model. It is significant that not only the separation between the surface and volume dependent kinetics is resolved clearly, but also the experimentally determined values of the dimensionless ratio versus X coincide closely with surface dependent nucleation behavior.

The significance of the agreement with surface dependent nucleation is emphasized by the fact that the experimental determinations of the dimensionless ratio are not required to follow either of the predicted kinetics paths. The predicted surface area or volume dependent path is established from independent stereological size distribution measurement. Thus, the close correspondence between two independent

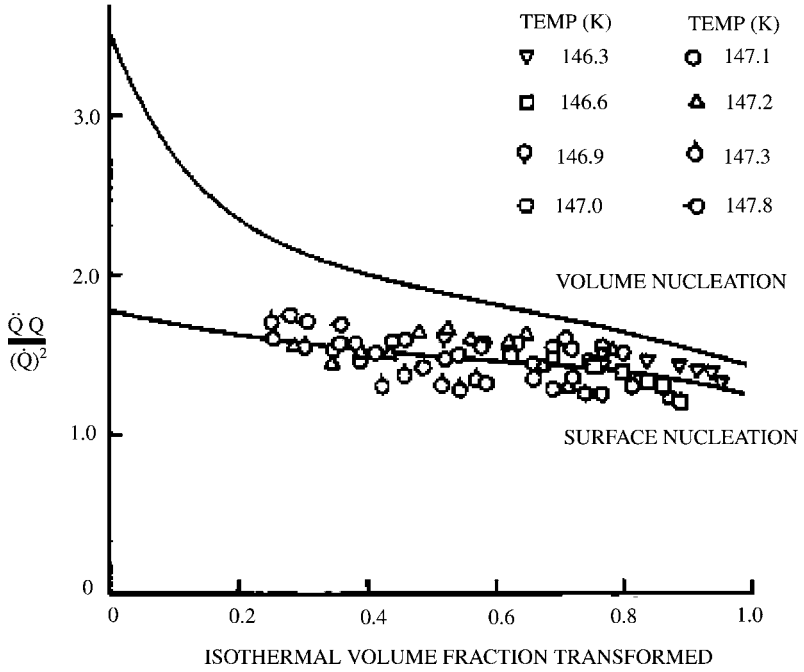

Fig. 7. Comparison of the experimental dimensionless ratio with the calculated value.

measurements from the same droplet sample provides a high degree of confidence in the outcome of the analysis which also agrees with the previous method [2]. When the possible uncertainties involved in each portion of the measurement are considered together, the relative uncertainty in assigning an experimental value for the dimensionless ratio is not expected to exceed 20%.

In terms of classical nucleation theory, surface area dependent nucleation rate may be expressed as follows:

$$J_a = K_a \exp\left[-\frac{16\pi\sigma^3 f(\theta)}{3kT(\Delta G_v)^2}\right] \quad (29)$$

where K_a is a prefactor, σ the liquid–solid interfacial energy, $f(\theta)$ the contact angle function for spherical cap nuclei [2], ΔG_v the driving free energy and kT has the usual meaning. Experimental J_a values for the samples examined from two sources are plotted in Fig. 8 as a function of temperature. It is noteworthy that the measurements of J_a for each sample in Fig. 8 are in good agreement. A fairly good linear relationship between $\log(J_a)$ and $1/T(\Delta G_v)^2$ is established when the measured values of ΔG_v are used for the analysis [15]. According to Fig. 8, the present results yield a composite slope which indicates a value of $\sigma f(\theta)^{1/3}$ of 31.3 mJ m^{-2} and an extrapolated value for K_a of $10^{39\pm2}$ cm^{-2} s^{-1}. The value for K_a calculated from the classical nucleation theory for a spherical sector is 10^{27} cm^{-2} s^{-1} which is in substantial disagreement with the value determined by experiments. This discrepancy may be removed as noted previously [2,3] if it is considered that the liquid–solid interface exhibits a negative entropy [16,17] for a constant $f(\theta)$. With the development of a droplet kinetics analysis that offers good resolution of the operating mechanism, a further analysis of the nucleation process is now in progress.

1.5.2. Nucleation catalysis

In the case of heterogeneous nucleation by a primary phase, nucleation occurs at the interface between the primary phase and the liquid. It is expected that changes in interface morphology will be reflected in the undercooling behavior. A schematic illustration of the thermal treatment employed to alter the primary phase morphology is shown in Fig. 9a for the Bi-rich portion of the Bi–Cd system. In this figure, T_{high} denotes the initial temperature for the liquid–solid combination, T_{het} is the nucleation temperature during a heterogeneous cycle and at T_{low} the samples is fully solid.

Several alloy systems, such as Bi–Cd and Sn–Sb, exhibit multiple nucleation exotherms upon cooling.

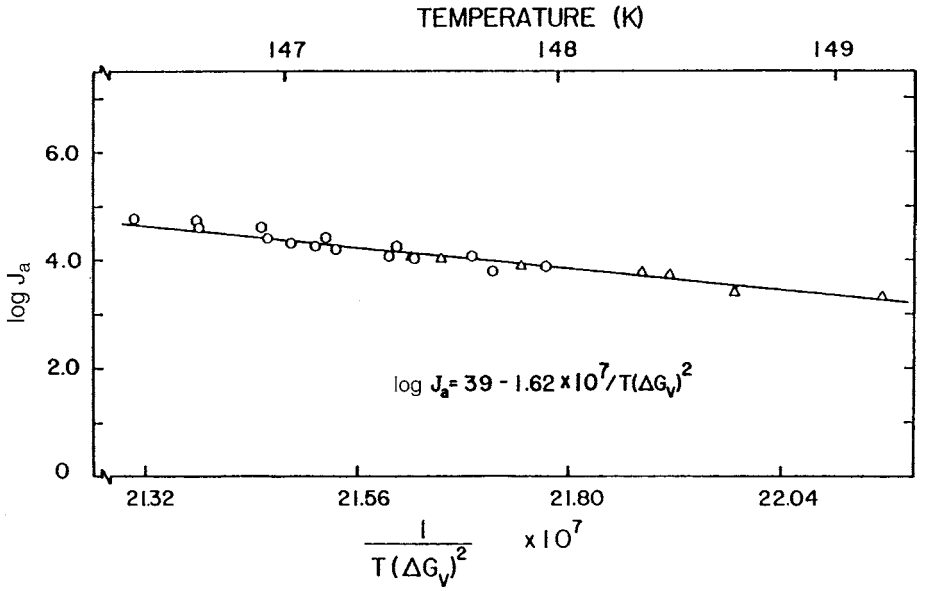

Fig. 8. Plot of $\log(J_a)$ as a function of $1/T(\Delta G_v)^2$ including results from different samples.

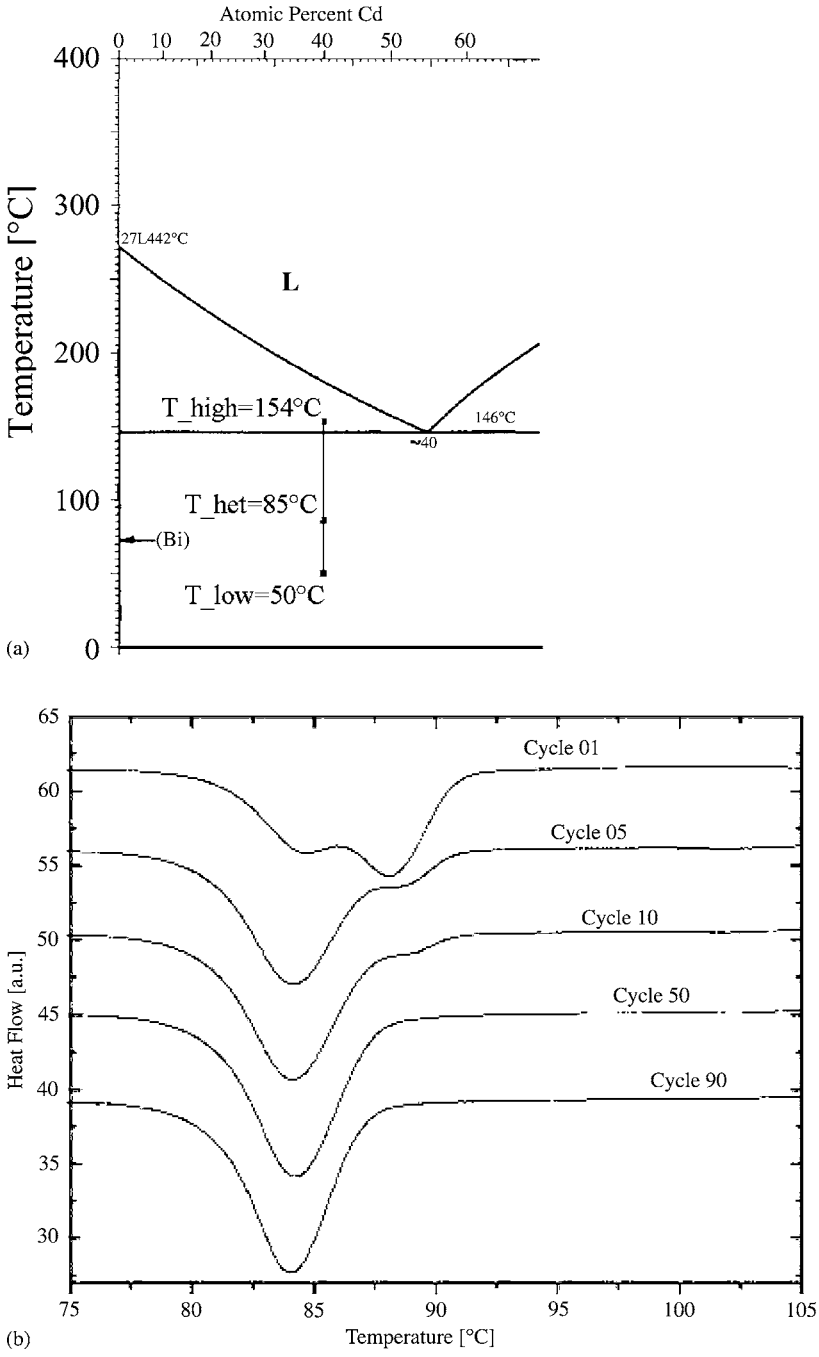

Fig. 9. (a) Heterogeneous cooling cycle design for a Bi–40 at.% Cd droplet sample. (b) Heterogeneous cooling cycles on a Bi–40 at.% Cd droplet population.

Upon repeated heterogeneous cycling, where partial remelting of the primary and complete melting of the secondary phase occurs, a shift in relative peak area between the respective exotherms is observed, indicating a change in relative site density of the different nucleation sites. For the Bi–Cd system (Fig. 9b), the first trace exhibits one very clear exothermic signal with only a small shoulder at high undercoolings. During consecutive cycles, a higher-undercooling peak develops from the small shoulder and, after only five cycles, contains most of the total heat evolved. After a total of 50 cycles, the initial situation is reversed, showing a very clear peak at high undercooling. Further cycling showed this nucleation response to be stable for at least 100 additional cycles so that isothermal crystallization measurements refer to identical sample conditions.

In several low-melting alloys, a transformation in primary phase particle morphology has been observed to occur simultaneous with this peak shift. While the initial droplets typically contain several irregularly shaped particles of the primary phase, the cycling behavior results in a facetting tendency that ultimately leads to a single primary phase particle with very clearly developed facets within each droplet. It is expected that the observed modification of substrate shape and the development of smooth, flat liquid–solid interfaces at the micron scale is reflected at the atomic scale in a similar structural configuration development. For example, a higher energy site involving multiple or defective steps can be progressively reduced in number with thermal cycling treatment. The example observed in Fig. 10 supports this type of behavior. In this sense, a quantitative nucleation kinetics analysis can offer an interfacial probe or diagnostic tool including dynamic effects.

Following the attainment of a stable nucleation response by repeated thermal cycling a series of isothermal measurements has been conducted to evaluate the catalysis of the Bi solid for the crystallization of Cd in a Bi–40 at.% Cd droplet sample. First the sample was heated to a temperature in the liquid+ solid two-phase field (i.e. T_{high}). It was then cooled to the isothermal holding temperature allowing for the determination of the fraction solidified prior to the attainment of the isothermal reaction temperature. The heat flow from a selection of isothermal treatments is shown as a function of holding time in Fig. 11 for

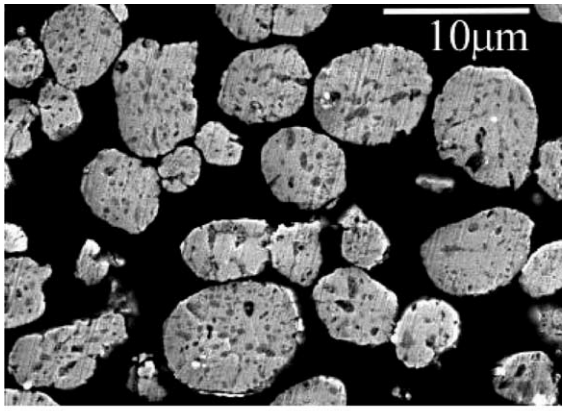

(a)

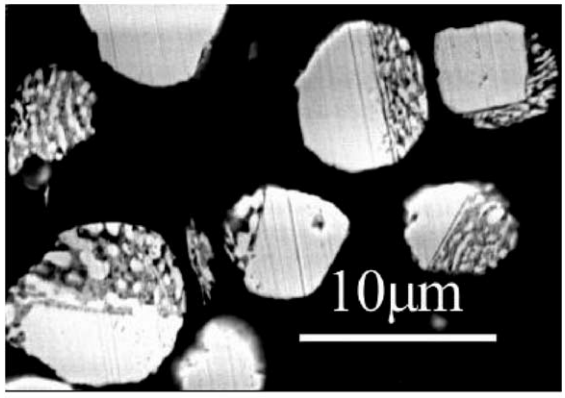

(b)

Fig. 10. Microstructure in Bi–40 at.% Cd droplets with the lighter Bi phase and the dark Cd: (a) as-emulsified; (b) after 30 heterogeneous cycles.

isotherms between 86 and 90 °C where accurate measurements are possible. For temperatures above 90 °C the nucleation rate is low. For temperatures below 86 °C the high nucleation rate yields a significant fraction crystallized before reaching the isotherm hold temperature and an initial transient at the onset of isothermal holding. The isothermal heat flow curves in Fig. 11 appear to follow a consistent pattern. From the measured droplet size distribution the nucleation rate can be evaluated based upon Eq. (16). The temperature dependence of J is given in Fig. 12 over the temperature range of measurement. Two linear portions are observed within the measurement range. For the low temperature portion from 86 to 88 °C the analysis in terms of Eq. (16) yields a prefactor of 5.5×10^{25} cm^{-2} s^{-1} which corresponds to a site

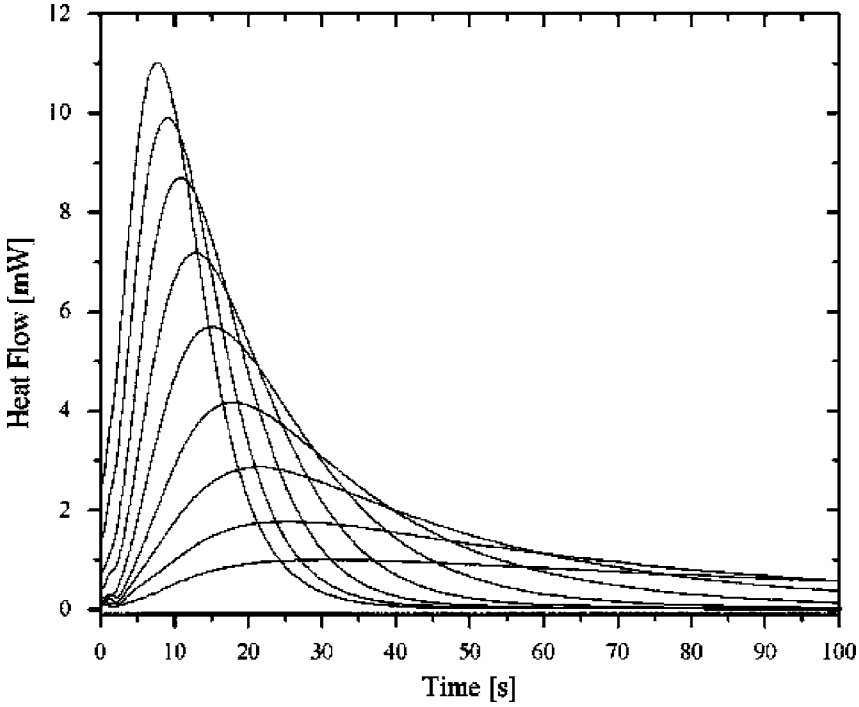

Fig. 11. Heat flow for the first 100 s for every fifth of the isothermal treatments between 86 and 90 °C. The highest peak represents the holding trace at 86 °C, whereas the lowest peak represents holding at 90 °C.

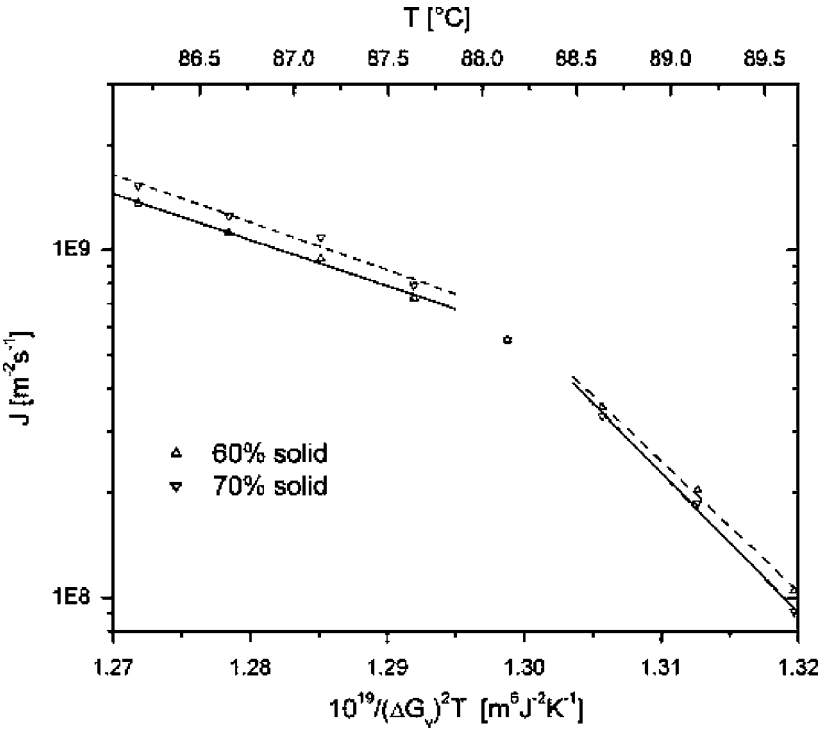

Fig. 12. Nucleation rate calculated from $\dot{Q}$ for two different solid fractions, with two linear fit parameter sets for each trace.

density of 5.7×10^{13} cm^{-2} and a value for $f(\theta)\sigma^3$ of 2.5×10^{-4} J^3 m^{-6}. These values are consistent with the classical nucleation theory. For the high temperature fit in Fig. 12 at temperatures above 88 °C, the prefactor and the corresponding site density are anomalously large for a single nucleation mechanism. Apparently, even though the continuous cooling traces in Fig. 9b suggest that thermal cycling has removed the high temperature peak, it is still present to confound the analysis of the nucleation kinetics. This result emphasizes the importance of isothermal measurements compared to continuous cooling runs to provide the resolution to separate kinetic processes that occur over nearly the same temperature range.

2. Summary

Nucleation is an important aspect in all transformations. Under most conditions, solidification is initiated by a heterogeneous nucleation event. While the study of homogeneous nucleation requires the sample free from all external nucleants, the study of heterogeneous nucleation requires a sample which contains only well known and characterized nucleants. A proper examination of nucleation catalysis requires the full identification of the catalytic site and solidification structure. In bulk systems, these requirements are extremely difficult to satisfy with certainty, since there exists a variety of potentially viable heterogeneous sites dispersed throughout the volume.

To circumvent the difficulties encountered in bulk systems, a droplet sample technique has been utilized to examine nucleation kinetics. In this approach a bulk liquid is dispersed into many fine droplets to limit the influence of extraneous nucleants. In order to evaluate the crystallization kinetics of droplet samples by DSC methods, it is essential to include the sample size distribution into the analysis of the calorimetric signal. By using droplet samples in peritectic or eutectic alloys that exhibit a high undercooling before nucleation and equilibrating the alloys in the liquid plus solid two-phase field, the catalytic effect of the different primary solids on subsequent nucleation of the liquid can be examined without the possible influence from a foreign substrate. With this approach, reproducible experimental studies of heterogeneous nucleation can be designed under well-defined conditions.

Acknowledgements

The support of the NSF (DMR-9712523) is gratefully acknowledged.

References

[1] J.H. Perepezko, Mater. Sci. Eng. A178 (1994) 105.
[2] D. Turnbull, J. Chem. Phys. 20 (1952) 411.
[3] Y. Miyazawa, G.M. Pound, J. Cryst. Growth 23 (1974) 45.
[4] D. Turnbull, R.L. Cormia, J. Chem. Phys. 34 (1961) 820.
[5] W.E. McMullen, D.W. Oxtoby, J. Chem. Phys. 88 (1988) 1967.
[6] K. Nishioka, H. Tomino, I. Kusaka, T. Takai, Phys. Rev. A 39 (1989) 772.
[7] E. Burke, J.Q. Brougnton, G.H. Gilmer, J. Chem. Phys. 89 (1988) 1030.
[8] J.H. Perepezko, Mater. Sci. Eng. 65 (1984) 125.
[9] D. Turnbull, J. Chem. Phys. 18 (1950) 198.
[10] M.E. Glicksmann, W.J. Childs, Acta. Metall. 10 (1962) 925.
[11] J.H. Perepezko, M.J. Uttormark, Met. Mater. Trans. A 27A (1996) 553.
[12] C.P. Tsokos, Probability Distribution: An Introduction to Probability Theory with Application, Duxbury Press, Belmont, CA, 1972.
[13] J.S. Paik, Ph.D. Thesis, University of Wisconsin, 1981.
[14] D. Turnbull, in: J.W. Christian, P. Haasen, T.B. Massalski (Eds.), Progress in Materials Science, Chalmers Ann. Vol., Pergamon Press, Oxford, UK, 1981, p. 269 (private communication).
[15] J.H. Perepezko, J.S. Paik, J. Non Cryst. Solids 61 (1984) 113.
[16] F. Spaepen, Acta Metall. 238 (1975) 729.
[17] F. Spaepen, Solid State Phys. 47 (1994) 1.